Advances in Applied Mathematics and Mechanics
Adv. Appl. Math. Mech., Vol. **5**, No. 3, pp. 351-364

DOI: 10.4208/aamm.11-m11176
June 2013

A New Higher Order Shear Deformation Model for Static Behavior of Functionally Graded Plates

Tahar Hassaine Daouadji[1,2,*], Abdelouahed Tounsi[2] and El Abbes Adda Bedia[2]

[1] *Université Ibn Khaldoun, BP 78 Zaaroura, 14000 Tiaret, Algérie*
[2] *Laboratoire des Matériaux & Hydrologie, Université de Sidi Bel Abbes, Algérie*

Received 16 November 2011; Accepted (in revised version) 10 October 2012

Available online 30 April 2013

Abstract. In this paper, a new displacement based high-order shear deformation theory is introduced for the static response of functionally graded plate. Unlike any other theory, the number of unknown functions involved is only four, as against five in case of other shear deformation theories. The theory presented is variationally consistent, has strong similarity with classical plate theory in many aspects, does not require shear correction factor, and gives rise to transverse shear stress variation such that the transverse shear stresses vary parabolically across the thickness satisfying shear stress free surface conditions. The mechanical properties of the plate are assumed to vary continuously in the thickness direction by a simple power-law distribution in terms of the volume fractions of the constituents. Numerical illustrations concerned flexural behavior of FG plates with Metal-Ceramic composition. Parametric studies are performed for varying ceramic volume fraction, volume fraction profiles, aspect ratios and length to thickness ratios. The validity of the present theory is investigated by comparing some of the present results with those of the classical, the first-order and the other higher-order theories. It can be concluded that the proposed theory is accurate and simple in solving the static behavior of functionally graded plates.

AMS subject classifications: 74K20

Key words: Functionally graded material, power law index, volume fraction, higher-order shear deformation theory, Navier solution.

1 Introduction

The concept of functionally graded materials (FGMs) were the first introduced in 1984 by a group of material scientists in Japan, as ultrahigh temperature resistant materials for air-

*Corresponding author.
Email: daouadjitah@yahoo.fr (T. Hassaine Daouadji)

 ©2013 Global Science Press

craft, space vehicles and other engineering applications. Functionally graded materials (FGMs) are new composite materials in which the micro-structural details are spatially varied through non-uniform distribution of the reinforcement phase. This is achieved by using reinforcement with different properties, sizes and shapes, as well as by interchanging the role of reinforcement and matrix phase in a continuous manner. The result is a microstructure that produces continuous or smooth change on thermal and mechanical properties at the macroscopic or continuum level (Koizumi, 1993 [1]; Hirai and Chen, 1999 [2]). Now, FGMs are developed for general use as structural components in extremely high temperature environments. Therefore, it is important to study the wave propagation of functionally graded materials structures in terms of non-destructive evaluation and material characterization.

Several studies have been performed to analyze the mechanical or the thermal or the thermo-mechanical responses of FG plates and shells. A comprehensive review is done by Tanigawa (1995) [3]. Reddy (2000) [4] has analyzed the static behavior of functionally graded rectangular plates based on his third-order shear deformation plate theory. Cheng and Batra (2000) [5] have related the deflections of a simply supported FG polygonal plate given by the first-order shear deformation theory and third-order shear deformation theory to that of an equivalent homogeneous Kirchhoff plate [6]. The static response of FG plate has been investigated by Zenkour (2006) [7] using a generalized shear deformation theory. In a recent study, şimşek (2010) [8] has studied the dynamic deflections and the stresses of an FG simply-supported beam subjected to a moving mass by using Euler-Bernoulli, Timoshenko and the parabolic shear deformation beam theory. şimşek (2010) [9] Benchour et al. [10] and Abdelaziz et al. 2010 [11] studied the free vibration of FG beams having different boundary conditions using the classical, the first-order and different higher-order shear deformation beam and plate theories. The non-linear dynamic analysis of a FG beam with pinned-pinned supports due to a moving harmonic load has been examined by şimşek (2010) [12] using Timoshenko beam theory.

The primary objective of this paper is to present a general formulation for functionally graded plates (FGP) using a new higher order shear deformation plate theory with only four unknown functions. The present theory satisfies equilibrium conditions at the top and bottom faces of the plate without using shear correction factors. The hyperbolic function in terms of thickness coordinate is used in the displacement field to account for shear deformation. Governing equations are derived from the principle of minimum total potential energy. Navier solution is used to obtain the closed-form solutions for simply supported FG plates. To illustrate the accuracy of the present theory, the obtained results are compared with three-dimensional elasticity solutions [13] and results of the first-order and the other higher-order theories (Table 1).

In this study, a new displacement models for an analysis of simply supported FGM plates are proposed. The plates are made of an isotropic material with material properties varying in the thickness direction only. Analytical solutions for bending deflections of FGM plates are obtained. The governing equations are derived from the principle of minimum total potential energy. Numerical examples are presented to illustrate the ac-

Table 1: Displacement models.

Model	Theory	Unknown function
CPT	Classical Plate Theory [6]	3
ATDSP	Analytical Tree Dimensional Solution for Plate (3-D) [13]	5
SSDPT	Sinusoidal Shear Deformation Plate Theory (Zenkour) [7]	5
PSDPT	Parabolic Shear Deformation Plate Theory (Reddy) [4]	5
NHPSDT	New Hyperbolic Shear Deformation Theory (present theory)	4

curacy and efficiency of the present theory by comparing the obtained results with those computed using various other theories.

2 Problem formulation

Consider a plate of total thickness h and composed of functionally graded material through the thickness (Fig. 1). It is assumed that the material is isotropic and grading is assumed to be only through the thickness. The xy plane is taken to be the undeformed mid plane of the plate with the z axis positive upward from the mid plane.

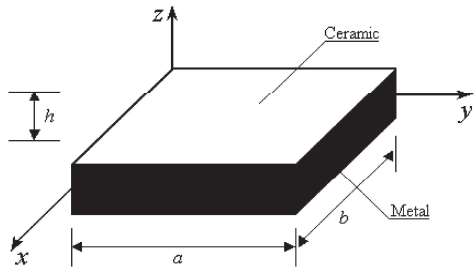

Figure 1: Geometry of rectangular plate composed of FGM.

2.1 Displacement fields and strains

The assumed displacement field is as follows:

$$\mathbf{u}(x,y,z)=\mathbf{u}_0(x,y)-z\frac{\partial \mathbf{w}_b}{\partial x}-f(z)\frac{\partial \mathbf{w}_s}{\partial x}, \tag{2.1a}$$

$$\mathbf{v}(x,y,z)=\mathbf{v}_0(x,y)-z\frac{\partial \mathbf{w}_b}{\partial y}-f(z)\frac{\partial \mathbf{w}_s}{\partial y}, \tag{2.1b}$$

$$\mathbf{w}(x,y,z)=\mathbf{w}_b(x,y)+\mathbf{w}_s(x,y), \tag{2.1c}$$

where $\mathbf{u}_0$ and $\mathbf{v}_0$ are the mid-plane displacements of the plate in the x and y direction, respectively; $\mathbf{w}_b$ and $\mathbf{w}_s$ are the bending and shear components of transverse displacement, respectively, while $f(z)$ represents shape functions (NHPSDT: New Hyperbolic

Shear Deformation Theory) determining the distribution of the transverse shear strains and stresses along the thickness and is given as:

$$f(z)=z-\left(z\mathrm{sec}h\left(\frac{\pi z^2}{h^2}\right)-z\mathrm{sec}h\left(\frac{\pi}{4}\right)\left(1-\frac{\pi}{2}\tanh\left(\frac{\pi}{4}\right)\right)\right). \tag{2.2}$$

It should be noted that unlike the first-order shear deformation theory, this theory does not require shear correction factors. The kinematic relations can be obtained as follows:

$$\varepsilon_x=\varepsilon_x^0+zk_x^b+f(z)k_x^s,\qquad \varepsilon_y=\varepsilon_y^0+zk_y^b+f(z)k_y^s,\qquad \gamma_{xy}=\gamma_{xy}^0+zk_{xy}^b+f(z)k_{xy}^s, \tag{2.3a}$$

$$\gamma_{yz}=g(z)\gamma_{yz}^s,\qquad \gamma_{xz}=g(z)\gamma_{xz}^s,\qquad \varepsilon_z=0, \tag{2.3b}$$

where

$$\varepsilon_x^0=\frac{\partial \mathbf{u}_0}{\partial x},\qquad k_x^b=-\frac{\partial^2 \mathbf{w}_b}{\partial x^2},\quad k_x^s=-\frac{\partial^2 \mathbf{w}_s}{\partial x^2},\qquad \varepsilon_y^0=\frac{\partial \mathbf{v}_0}{\partial y}, \tag{2.4a}$$

$$k_y^b=-\frac{\partial^2 \mathbf{w}_b}{\partial y^2},\qquad k_y^s=-\frac{\partial^2 \mathbf{w}_s}{\partial y^2},\quad \gamma_{xy}^0=\frac{\partial \mathbf{u}_0}{\partial y}+\frac{\partial \mathbf{v}_0}{\partial x},\quad k_{xy}^b=-2\frac{\partial^2 \mathbf{w}_b}{\partial x\partial y}, \tag{2.4b}$$

$$k_{xy}^s=-2\frac{\partial^2 \mathbf{w}_s}{\partial x\partial y},\quad \gamma_{yz}^s=\frac{\partial \mathbf{w}_s}{\partial y},\qquad \gamma_{xz}^s=\frac{\partial \mathbf{w}_s}{\partial x},\quad g(z)=1-f'(z)\quad\text{and}\quad f'(z)=\frac{df(z)}{dz}. \tag{2.4c}$$

2.2 Constitutive relations

In FGM, material property gradation is considered through the thickness and the expression given below represents the profile for the volume fraction

$$P(z)=(P_t-P_b)\left(\frac{z}{h}+\frac{1}{2}\right)^k+P_b, \tag{2.5a}$$

$$E(z)=(E_t-E_b)\left(\frac{z}{h}+\frac{1}{2}\right)^k+E_b, \tag{2.5b}$$

$$G(z)=(G_t-G_b)\left(\frac{z}{h}+\frac{1}{2}\right)^k+G_b, \tag{2.5c}$$

where P denotes a generic material property like modulus, P_t and P_b denotes the property of the top and bottom faces of the plate respectively, and k is a parameter that dictates material variation profile through the thickness. Here, it is assumed that modules $E(z)$ and $G(z)$ vary according to Eq. (2.5) and ν is assumed to be a constant. The linear constitutive relations are

$$\begin{Bmatrix}\sigma_x\\ \sigma_y\\ \tau_{yz}\\ \tau_{xz}\\ \tau_{xy}\end{Bmatrix}=\begin{bmatrix}Q_{11} & Q_{12} & 0 & 0 & 0\\ Q_{12} & Q_{11} & 0 & 0 & 0\\ 0 & 0 & Q_{44} & 0 & 0\\ 0 & 0 & 0 & Q_{55} & 0\\ 0 & 0 & 0 & 0 & Q_{66}\end{bmatrix}\begin{Bmatrix}\varepsilon_x\\ \varepsilon_y\\ \gamma_{yz}\\ \gamma_{xz}\\ \gamma_{xy}\end{Bmatrix}, \tag{2.6}$$

where

$$Q_{11}=\frac{E(z)}{1-\nu^2},\qquad Q_{12}=\nu Q_{11},\qquad Q_{44}=Q_{55}=Q_{66}=\frac{E(z)}{2(1+\nu)}. \tag{2.7}$$

2.3 Governing equations

The governing equations of equilibrium can be derived by using the principle of virtual displacements. The principle of virtual work in the present case yields

$$\int_{-h/2}^{h/2}\int_{\Omega}\left[\sigma_x\delta\varepsilon_x+\sigma_y\delta\varepsilon_y+\tau_{xy}\delta\gamma_{xy}+\tau_{yz}\delta\gamma_{yz}+\tau_{xz}\delta\gamma_{xz}\right]d\Omega dz-\int_{\Omega}q\delta w d\Omega=0, \tag{2.8}$$

where Ω is the top surface and q is the applied transverse load.

Substituting Eqs. (2.3) and (2.6) into Eq. (2.8) and integrating through the thickness of the plate, Eq. (2.8) can be rewritten as

$$\begin{aligned}\int_{\Omega}\big[&N_x\delta\varepsilon_x^0+N_y\delta\varepsilon_y^0+N_{xy}\delta\varepsilon_{xy}^0+M_x^b\delta k_x^b+M_y^b\delta k_y^b+M_{xy}^b\delta k_{xy}^b+M_x^s\delta k_x^s\\&+M_y^s\delta k_y^s+M_{xy}^s\delta k_{xy}^s+S_{yz}^s\delta\gamma_{yz}^s+S_{xz}^s\delta\gamma_{xz}^s\big]d\Omega-\int_{\Omega}q\delta w d\Omega=0,\end{aligned} \tag{2.9}$$

where

$$\begin{Bmatrix}N_x & N_y & N_{xy}\\ M_x^b & M_y^b & M_{xy}^b\\ M_x^s & M_y^s & M_{xy}^s\end{Bmatrix}=\int_{-h/2}^{h/2}(\sigma_x,\sigma_y,\tau_{xy})\begin{Bmatrix}1\\ z\\ f(z)\end{Bmatrix}dz, \tag{2.10a}$$

$$(S_{xz}^s,S_{yz}^s)=\int_{-h/2}^{h/2}(\tau_{xz},\tau_{yz})g(z)dz. \tag{2.10b}$$

The governing equations of equilibrium can be derived from Eq. (2.9) by integrating the displacement gradients by parts and setting the coefficients $\delta\mathbf{u}_0$, $\delta\mathbf{v}_0$, $\delta\mathbf{w}_b$ and $\delta\mathbf{w}_s$ zero separately. Thus one can obtain the equilibrium equations associated with the present shear deformation theory,

$$\delta\mathbf{u}:\ \frac{\partial N_x}{\partial x}+\frac{\partial N_{xy}}{\partial y}=0, \tag{2.11a}$$

$$\delta\mathbf{v}:\ \frac{\partial N_{xy}}{\partial x}+\frac{\partial N_y}{\partial y}=0, \tag{2.11b}$$

$$\delta\mathbf{w}_b:\ \frac{\partial^2 M_x^b}{\partial x^2}+2\frac{\partial^2 M_{xy}^b}{\partial x\partial y}+\frac{\partial^2 M_y^b}{\partial y^2}+q=0, \tag{2.11c}$$

$$\delta\mathbf{w}_s:\ \frac{\partial^2 M_x^s}{\partial x^2}+2\frac{\partial^2 M_{xy}^s}{\partial x\partial y}+\frac{\partial^2 M_y^s}{\partial y^2}+\frac{\partial S_{xz}^s}{\partial x}+\frac{\partial S_{yz}^s}{\partial y}+q=0. \tag{2.11d}$$

Using Eq. (2.6) in Eq. (2.10), the stress resultants of a plate made up of three layers can be related to the total strains by

$$\begin{Bmatrix} N \\ M^b \\ M^s \end{Bmatrix} = \begin{bmatrix} A & B & B^s \\ A & D & D^s \\ B^s & D^s & H^s \end{bmatrix} \begin{Bmatrix} \varepsilon \\ k^b \\ k^s \end{Bmatrix}, \qquad S = A^s \gamma, \tag{2.12}$$

where

$$N = \{N_x, N_y, N_{xy}\}^t, \qquad M^b = \{M^b_x, M^b_y, M^b_{xy}\}^t, \qquad M^s = \{M^s_x, M^s_y, M^s_{xy}\}^t, \tag{2.13a}$$

$$\varepsilon = \{\varepsilon^0_x, \varepsilon^0_y, \gamma^0_{xy}\}^t, \qquad k^b = \{k^b_x, k^b_y, k^b_{xy}\}^t, \qquad k^s = \{k^s_x, k^s_y, k^s_{xy}\}^t, \tag{2.13b}$$

$$A = \begin{bmatrix} A_{11} & A_{12} & 0 \\ A_{12} & A_{22} & 0 \\ 0 & 0 & A_{66} \end{bmatrix}, \quad B = \begin{bmatrix} B_{11} & B_{12} & 0 \\ B_{12} & B_{22} & 0 \\ 0 & 0 & B_{66} \end{bmatrix}, \quad D = \begin{bmatrix} D_{11} & D_{12} & 0 \\ D_{12} & D_{22} & 0 \\ 0 & 0 & D_{66} \end{bmatrix}, \tag{2.13c}$$

$$B^s = \begin{bmatrix} B^s_{11} & B^s_{12} & 0 \\ B^s_{12} & B^s_{22} & 0 \\ 0 & 0 & B^s_{66} \end{bmatrix}, \quad D^s = \begin{bmatrix} D^s_{11} & D^s_{12} & 0 \\ D^s_{12} & D^s_{22} & 0 \\ 0 & 0 & D^s_{66} \end{bmatrix}, \quad H^s = \begin{bmatrix} H^s_{11} & H^s_{12} & 0 \\ H^s_{12} & H^s_{22} & 0 \\ 0 & 0 & H^s_{66} \end{bmatrix}, \tag{2.13d}$$

$$S = \{S^s_{xz}, S^s_{yz}\}^t, \qquad \gamma = \{\gamma_{xz}, \gamma_{yz}\}^t, \qquad A^s = \begin{bmatrix} A^s_{44} & 0 \\ 0 & A^s_{55} \end{bmatrix}, \tag{2.13e}$$

where A_{ij}, B_{ij}, etc., are the plate stiffness, defined by

$$\begin{Bmatrix} A_{11} & B_{11} & D_{11} & B^s_{11} & D^s_{11} & H^s_{11} \\ A_{12} & B_{12} & D_{12} & B^s_{12} & D^s_{12} & H^s_{12} \\ A_{66} & B_{66} & D_{66} & B^s_{66} & D^s_{66} & H^s_{66} \end{Bmatrix}$$
$$= \int_{-h/2}^{h/2} Q_{11} \left(1, z, z^2, f(z), zf(z), f^2(z)\right) \begin{Bmatrix} 1 \\ \nu \\ \dfrac{1-\nu}{2} \end{Bmatrix} dz, \tag{2.14a}$$

and

$$(A_{22}, B_{22}, D_{22}, B^s_{22}, D^s_{22}, H^s_{22}) = (A_{11}, B_{11}, D_{11}, B^s_{11}, D^s_{11}, H^s_{11}), \tag{2.14b}$$

$$A^s_{44} = A^s_{55} = \int_{h_{n-1}}^{h_n} Q_{44} [g(z)]^2 dz. \tag{2.14c}$$

Substituting from Eq. (2.12) into Eq. (2.11), we obtain the following equation,

$$\begin{aligned} &A_{11} d_{11} \mathbf{u}_0 + A_{66} d_{22} \mathbf{u}_0 + (A_{12} + A_{66}) d_{12} \mathbf{v}_0 - B_{11} d_{111} \mathbf{w}_b - (B_{12} + 2B_{66}) d_{122} \mathbf{w}_b \\ &\quad - (B^s_{12} + 2B^s_{66}) d_{122} \mathbf{w}_s - B^s_{11} d_{111} \mathbf{w}_s = 0, \end{aligned} \tag{2.15a}$$

$$\begin{aligned} &A_{22} d_{22} \mathbf{v}_0 + A_{66} d_{11} \mathbf{v}_0 + (A_{12} + A_{66}) d_{12} \mathbf{u}_0 - B_{22} d_{222} \mathbf{w}_b - (B_{12} + 2B_{66}) d_{112} \mathbf{w}_b \\ &\quad - (B^s_{12} + 2B^s_{66}) d_{112} \mathbf{w}_s - B^s_{22} d_{222} \mathbf{w}_s = 0, \end{aligned} \tag{2.15b}$$

$$\begin{aligned}
&B_{11}d_{111}\mathbf{u}_0+(B_{12}+2B_{66})d_{122}\mathbf{u}_0+(B_{12}+2B_{66})d_{112}\mathbf{v}_0+B_{22}d_{222}\mathbf{v}_0-D_{11}d_{1111}\mathbf{w}_b\\
&\qquad -2(D_{12}+2D_{66})d_{1122}\mathbf{w}_b-D_{22}d_{2222}\mathbf{w}_b-D^s_{11}d_{1111}\mathbf{w}_s\\
&\qquad -2(D^s_{12}+2D^s_{66})d_{1122}\mathbf{w}_s-D^s_{22}d_{2222}\mathbf{w}_s=q, \qquad (2.15c)\\
&B^s_{11}d_{111}\mathbf{u}_0+(B^s_{12}+2B^s_{66})d_{122}\mathbf{u}_0+(B^s_{12}+2B^s_{66})d_{112}\mathbf{v}_0+B^s_{22}d_{222}\mathbf{v}_0-D^s_{11}d_{1111}\mathbf{w}_b\\
&\qquad -2(D^s_{12}+2D^s_{66})d_{1122}\mathbf{w}_b-D^s_{22}d_{2222}\mathbf{w}_b-H^s_{11}d_{1111}\mathbf{w}_s\\
&\qquad -2(H^s_{12}+2H^s_{66})d_{1122}\mathbf{w}_s-H^s_{22}d_{2222}\mathbf{w}_s+A^s_{55}d_{11}\mathbf{w}_s+A^s_{44}d_{22}\mathbf{w}_s=q. \qquad (2.15d)
\end{aligned}$$

Where d_{ij}, d_{ijl} and d_{ijlm} are the following differential operators:

$$d_{ij}=\frac{\partial^2}{\partial x_i\partial x_j},\quad d_{ijl}=\frac{\partial^3}{\partial x_i\partial x_j\partial x_l},\quad d_{ijlm}=\frac{\partial^4}{\partial x_i\partial x_j\partial x_l\partial x_m},\quad d_i=\frac{\partial}{\partial x_i},\quad (i,j,l,m=1,2). \qquad (2.16)$$

2.4 Exact solution for a simply-supported FGM plate

Rectangular plates are generally classified in accordance with the type of support used. We are here concerned with the exact solution of Eqs. (2.15a)-(2.15d) for a simply supported FG plate. The following boundary conditions are imposed at the side edges:

$$\mathbf{v}_0=\mathbf{w}_b=\mathbf{w}_s=\frac{\partial \mathbf{w}_s}{\partial y}=N_x=M^b_x=M^s_x=0 \qquad \text{at } x=-a/2,\ a/2, \qquad (2.17a)$$

$$\mathbf{u}_0=\mathbf{w}_b=\mathbf{w}_s=\frac{\partial \mathbf{w}_s}{\partial x}=N_y=M^b_y=M^s_y=0 \qquad \text{at } y=-b/2,\ b/2. \qquad (2.17b)$$

To solve this problem, Navier assumed that the transverse mechanical and temperature loads, q in the form of a double trigonometric series as

$$q=q_0\sin(\lambda x)\sin(\mu y), \qquad (2.18)$$

where $\lambda=\pi/a$, $\mu=\pi/b$ and q_0 represents the intensity of the load at the plate center.

Following the Navier solution procedure, we assume the following solution form for $\mathbf{u}_0$, $\mathbf{v}_0$, $\mathbf{w}_b$ and $\mathbf{w}_s$ that satisfies the boundary conditions,

$$\begin{Bmatrix}\mathbf{u}_0\\ \mathbf{v}_0\\ \mathbf{w}_b\\ \mathbf{w}_s\end{Bmatrix}=\begin{Bmatrix}\mathbf{U}\cos(\lambda x)\sin(\mu y)\\ \mathbf{V}\sin(\lambda x)\cos(\mu y)\\ \mathbf{W}_b\sin(\lambda x)\sin(\mu y)\\ \mathbf{W}_s\sin(\lambda x)\sin(\mu y)\end{Bmatrix}, \qquad (2.19)$$

where $\mathbf{U}$, $\mathbf{V}$, $\mathbf{W}_b$ and $\mathbf{W}_s$ are arbitrary parameters to be determined subjected to the condition that the solution in Eq. (2.19) satisfies governing Eqs. (2.15). One obtains the following operator equation,

$$[C]\{\Delta\}=\{P\}, \qquad (2.20)$$

where $\{\Delta\}=\{\mathbf{U},\mathbf{V},\mathbf{W}_b,\mathbf{W}_s\}^t$ and $[C]$ is the symmetric matrix given by

$$[C]=\begin{bmatrix} a_{11} & a_{12} & a_{13} & a_{14} \\ a_{12} & a_{22} & a_{23} & a_{24} \\ a_{13} & a_{23} & a_{33} & a_{34} \\ a_{14} & a_{24} & a_{34} & a_{44} \end{bmatrix}, \tag{2.21}$$

in which

$$a_{11}=A_{11}\lambda^2+A_{66}\mu^2, \qquad a_{12}=\lambda\mu(A_{12}+A_{66}), \tag{2.22a}$$

$$a_{13}=-\lambda[B_{11}\lambda^2+(B_{12}+2B_{66})\mu^2], \qquad a_{14}=-\lambda[B^s_{11}\lambda^2+(B^s_{12}+2B^s_{66})\mu^2], \tag{2.22b}$$

$$a_{22}=A_{66}\lambda^2+A_{22}\mu^2, \qquad a_{23}=-\mu[(B_{12}+2B_{66})\lambda^2+B_{22}\mu^2], \tag{2.22c}$$

$$a_{24}=-\mu[(B^s_{12}+2B^s_{66})\lambda^2+B^s_{22}\mu^2], \tag{2.22d}$$

$$a_{33}=D_{11}\lambda^4+2(D_{12}+2D_{66})\lambda^2\mu^2+D_{22}\mu^4, \tag{2.22e}$$

$$a_{34}=D^s_{11}\lambda^4+2(D^s_{12}+2D^s_{66})\lambda^2\mu^2+D^s_{22}\mu^4, \tag{2.22f}$$

$$a_{44}=H^s_{11}\lambda^4+2(H^s_{11}+2H^s_{66})\lambda^2\mu^2+H^s_{22}\mu^4+A^s_{55}\lambda^2+A^s_{44}\mu^2. \tag{2.22g}$$

3 Numerical results and discussions

The study has been focused on the static behavior of functionally graded plate based on the present new higher order shear deformation model. Here some representative results of the Navier solution obtained for a simply supported rectangular plate are presented.

A functionally graded material consisting of Aluminum-Alumina is considered. The following material properties are used in computing the numerical values (Bouazza al. [14]).

- Metal (Aluminium, Al): $E_M=70\text{GPa}, \quad \nu=0.3.$
- Ceramic (Alumina, Al_2O_3): $E_C=380\text{GPa}, \quad \nu=0.3.$

Now, a functionally graded material consisting of aluminum and alumina is considered. Young's modulus for aluminum is 70GPa while for alumina is 380GPa. Note that, Poisson's ratio is selected constant for both and equal to 0.3. The various non-dimensional parameters used are

$$\bar{w}=\frac{10h^3Ec}{a^4q_0}w\Big(\frac{a}{2},\frac{b}{2}\Big), \quad \bar{u}_x=\frac{100h^3Ec}{a^4q_0}u_x\Big(\frac{a}{2},\frac{b}{2},-\frac{h}{4}\Big), \quad \bar{u}_y=\frac{100h^3Ec}{a^4q_0}u_y\Big(\frac{a}{2},\frac{b}{2},-\frac{h}{6}\Big), \tag{3.1a}$$

$$\bar{\sigma}_x=\frac{h}{aq_0}\sigma_x\Big(\frac{a}{2},\frac{b}{2},\frac{h}{2}\Big), \quad \bar{\sigma}_y=\frac{h}{aq_0}\sigma_y\Big(\frac{a}{2},\frac{b}{2},\frac{h}{3}\Big), \tag{3.1b}$$

$$\bar{\tau}_{xy}=\frac{h}{aq_0}\tau_{xy}\Big(0,0,-\frac{h}{3}\Big), \quad \bar{\tau}_{yz}=\frac{h}{aq_0}\tau_{yz}\Big(\frac{a}{2},0,\frac{h}{6}\Big), \quad \bar{\tau}_{xz}=\frac{h}{aq_0}\tau_{xz}\Big(0,\frac{b}{2},0\Big). \tag{3.1c}$$

It is clear that the deflection increases as the side-to-thickness ratio decreases. The same results were obtained in most literatures. In addition, the correlation between the present new higher order shear deformation theory and different higher-order and first-order shear deformation theories is established by the author in his recent papers. It is found that this theory predicts the deflections and stresses more accurately when compared to the first and third-order theories.

For the sake of completeness, results of the present theory are compared with those obtained using a new Navier-type three-dimensionally exact solution for small deflections in bending of linear elastic isotropic homogeneous rectangular plates. The center deflection **w** and the distribution across the plate thickness of in-plane longitudinal stress σ_x and longitudinal tangential stress τ_{xy} are compared with the results of the 3-D solution and are shown in Tables 2 and 3. The present solution is realized for a quadratic plate, with the following fixed data: $a=1$, $b=1$, $E_m=E_c=E=1$, $q_0=1$, $\nu=0.3$ and three values

Table 2: Center deflections of isotropic homogenous plates ($k=0$, $E_m=E_c=E=1$ and $a/b=1$).

h/a	CPT	3D	SSDPT	NHPSDT	Reddy
		z=0		Present theory	
0.01	44360.9	44384.7	44383.84	44383.86	44383.87
0.03	1643.00	1650.94	1650.646	1650.652	1650.657
0.1	44.3609	46.7443	46.6548	46.65655	46.65836

Table 3: Distribution of stresses across the thickness of isotropic homogenous plates ($E_m=E_c=E=1$, $a/b=1$ and $k=0$).

h/a	z	$\sigma_x(a/2,b/2,z)$				$\tau_{xy}(0,0,-z)$			
		3D	SSDPT	NHPSDT Present	Reddy	3D	SSDPT	NHPSDT Present	Reddy
0.01	0.005	2873.3	2873.39	2873.422	2873.41	1949.6	1949.36	1949.086	1949.06
	0.004	2298.6	2298.57	2298.597	2298.593	1559.2	1559.04	1558.854	1558.84
	0.003	1723.9	1723.84	1723.861	1723.865	1169.1	1168.99	1168.883	1168.89
	0.002	1149.2	1149.18	1149.197	1149.205	779.3	779.18	779.127	779.151
	0.001	574.6	574.58	574.585	574.591	389.6	389.55	389.523	389.541
	0.000	0.000	0.000	0.00000	0.000	0.000	0.000	0.000	0.000
0.03	0.015	319.4	319.445	319.445	319.437	217.11	217.156	217.082	217.058
	0.012	255.41	255.415	255.416	255.413	173.26	173.282	173.255	173.244
	0.009	191.49	191.472	191.475	191.48	129.75	129.682	129.686	129.698
	0.006	127.63	127.603	127.607	127.615	86.41	86.313	86.330	86.354
	0.003	63.8	63.788	63.790	63.796	43.18	43.72	43.126	43.143
	0.000	0.000	0.000	0.0000	0.000	0.000	0.000	0.000	0.000
0.10	0.05	28.89	28.9307	28.928	28.92	19.92	20.0476	20.021	20.003
	0.04	22.998	23.0055	23.004	23.000	15.606	15.6459	15.638	15.629
	0.03	17.182	17.166	17.167	17.171	11.558	11.4859	11.494	11.504
	0.02	11.423	11.3994	11.402	11.410	7.642	7.5315	7.546	7.565
	0.01	5.702	5.6858	5.687	5.693	3.803	3.7265	3.7369	3.751
	0.00	0.000	0.000	0.000	0.000	0.000	0.000	0.000	0.000

Table 4: Effects of volume fraction exponent and loading on the dimensionless stresses and displacements of a FGM square plate $(a/h=10)$.

k	Theory	w	σ_x	σ_y	τ_{yz}	τ_{xz}	τ_{xy}
0	NHPSDT–Present	0.4665	2.8928	1.9104	0.4424	0.5072	1.2851
ceramic	SSDPT	0.4665	2.8932	1.9103	0.4429	0.5114	1.2850
	Reddy	0.4665	2.8920	1.9106	0.4411	0.4963	1.2855
	NHPSDT–Present	0.9421	4.2607	2.2569	0.54404	0.50721	1.1573
1	SSDPT	0.9287	4.4745	2.1692	0.5446	0.5114	1.1143
	Reddy	0.94214	4.25982	2.25693	0.54246	0.49630	1.15725
	NHPSDT–Present	1.2228	4.8890	2.1663	0.5719	0.4651	1.0448
2	SSDPT	1.1940	5.2296	2.0338	0.5734	0.4700	0.9907
	Reddy	1.22275	4.88814	2.16630	0.56859	0.45384	1.04486
	NHPSDT–Present	1.3533	5.2064	1.9922	0.56078	0.4316	1.0632
3	SSDPT	1.3200	5.6108	1.8593	0.5629	0.4367	1.0047
	Reddy	1.3530	5.20552	1.99218	0.55573	0.41981	1.06319
	NHPSDT–Present	1.4653	5.7074	1.7143	0.50075	0.4128	1.1016
5	SSDPT	1.4356	6.1504	1.6104	0.5031	0.4177	1.0451
	Reddy	1.46467	5.70653	1.71444	0.49495	0.40039	1.10162
	NHPSDT–Present	1.6057	6.9547	1.3346	0.4215	0.4512	1.1118
10	SSDPT	1.5876	7.3689	1.2820	0.4227	0.4552	1.0694
	Reddy	1.60541	6.95396	1.33495	0.41802	0.43915	1.1119
	NHPSDT–Present	2.5327	2.8928	1.9104	0.4424	0.5072	1.2851
∞	SSDPT	2.5327	2.8932	1.9103	0.4429	0.5114	1.2850
métal	Reddy	2.5328	2.8920	1.9106	0.4411	0.4963	1.2855

for the plate thickness: $h=0.01$, $h=0.03$ and $h=0.1$. It is to be noted that the present results compare very well with the 3-D solution. All deflections again compare well with the 3-D solution, and show good convergence with the average 3-D solution.

In Table 4, the effect of volume fraction exponent on the dimensionless stresses and displacements of a FGM square plate $(a/h=10)$ is given. This table shows comparison between results for plates subjected to uniform or sinusoidal distributed loads, respectively. As it is well known, the uniform load distribution always over predicts the displacements and stresses magnitude. As the plate becomes more and more metallic, the difference increases for deflection **w** and in-plane longitudinal stress σ_x, while it decreases for in-plane normal stress σ_y. It is important to observe that the stresses for a fully ceramic plate are the same as that for a fully metal plate. This is because the plate for these two cases is fully homogeneous and the stresses do not depend on the modulus of elasticity. Results in Table 4 should serve as benchmark results for future comparisons.

Tables 5 and 6 compares the deflections and stresses of different types of the FGM square plate $(a/b=1,\ k=0)$ and FGM rectangular plate $(b=3a,\ k=2)$. The deflections decrease as the aspect ratio a/b increases and this irrespective of the type of the FGM plate. All theories (SSDPT, PSDPT and NHPSDT) give the same axial stress σ_x and σ_y for a fully ceramic plate $(k=0)$. In general, the axial stress increases with the volume fraction exponent k. The transverse shear stress for a FGM plate subjected to a distributed load.

Table 5: Comparison of normalized displacements and stresses of a FGM square plate $(a/b=1)$, $k=0$.

a/h	Theory	w	σ_x	σ_y	τ_{yz}	τ_{xz}	τ_{xy}
4	NHPSDT–Present	0.5866	1.1979	0.7536	0.4307	0.4937	0.4908
	SSDPT	0.5865	1.1988	0.7534	0.4307	0.4973	0.4906
	Reddy	0.5868	1.1959	0.7541	0.4304	0.4842	0.4913
10	NHPSDT–Present	0.4665	2.8928	1.9104	0.4424	0.5072	1.2851
	SSDPT	0.4665	2.8932	1.9103	0.4429	0.5114	1.2850
	Reddy	0.4666	2.8920	1.9106	0.4411	0.4963	1.2855
100	NHPSDT–Present	0.4438	28.7342	19.1543	0.4466	0.5119	12.9884
	SSDPT	0.4438	28.7342	19.1543	0.4472	0.5164	13.0125
	Reddy	0.4438	28.7341	19.1543	0.4448	0.5004	12.9885

Table 6: Comparison of normalized displacements and stresses of a FGM rectangular plate $(b=3a)$ and $k=2$.

a/h	Theory	w	σ_x	σ_y	τ_{yz}	τ_{xz}	τ_{xy}
4	NHPSDT–Present	4.0569	5.2804	0.6644	0.6084	0.6699	0.5900
	SSDPT	3.99	5.3144	0.6810	0.6096	0.6796	0.5646
	Reddy	4.0529	5.2759	0.6652	0.6058	0.6545	0.5898
10	NHPSDT–Present	3.5543	12.9252	1.6938	0.61959	0.6841	1.4898
	SSDPT	3.5235	12.9374	1.7292	0.6211	0.6910	1.4500
	Reddy	3.5537	12.9234	1.6941	0.6155	0.6672	1.4898
20	NHPSDT–Present	3.4824	25.7712	3.3971	0.6214	0.6878	2.9844
	SSDPT	3.4567	25.7748	3.4662	0.6232	0.6947	2.9126
	Reddy	3.48225	25.7703	3.3972	0.6171	0.6704	2.9844
100	NHPSDT–Present	3.4593	128.728	17.0009	0.6220	0.6894	14.9303
	SSDPT	3.4353	128.713	17.3437	0.6238	0.6963	14.584
	Reddy	3.45937	128.7283	17.0009	0.6177	0.67176	14.9303

The results show that the transverse shear stresses may be indistinguishable. As the volume fraction exponent increases for FGM plates, the shear stress will increase and the fully ceramic plates give the smallest shear stresses.

Figs. 2 and 3 show the variation of the center deflection with the aspect and side-to-thickness ratios, respectively. The deflection is maximum for the metallic plate and minimum for the ceramic plate. The difference increases as the aspect ratio increases while it may be unchanged with the increase of side-to-thickness ratio. One of the main inferences from the analysis is that the response of FGM plates is intermediate to that of the ceramic and metal homogeneous plates (see also Table 4). It is to be noted that, in the case of thermal or combined loads and under certain conditions, the above response is not intermediate.

Figs. 4-5 depict the through-the-thickness distributions of the shear stresses τ_{yz} and τ_{xz} the inplane the longitudinal tangential stress τ_{xy} in the FGM plate under the uniform load. The volume fraction exponent of the FGM plate is taken as k=2 in these figures. Dis-

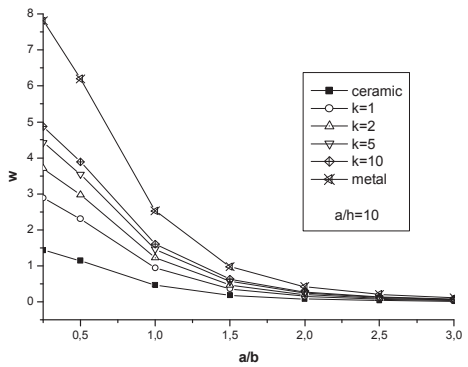

Figure 2: Dimensionless center deflection as function of the aspect ratio (a/b) of an FGM plate.

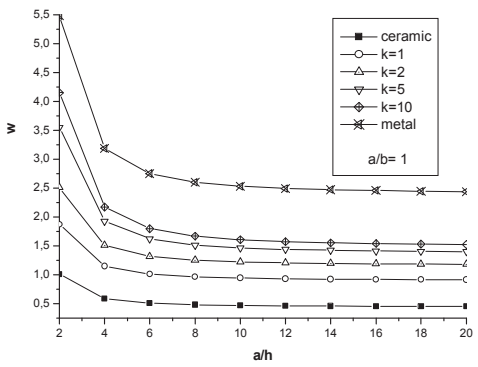

Figure 3: Dimensionless center deflection as a function of the side-to-thickness ratio (a/h) of an FGM plate.

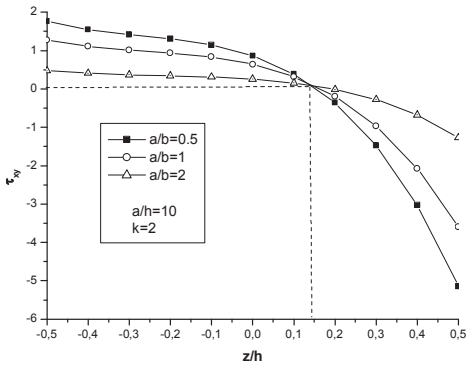

Figure 4: Variation of longitudinal tangential stress (τ_{xy}) through-the thickness of an FGM plate.

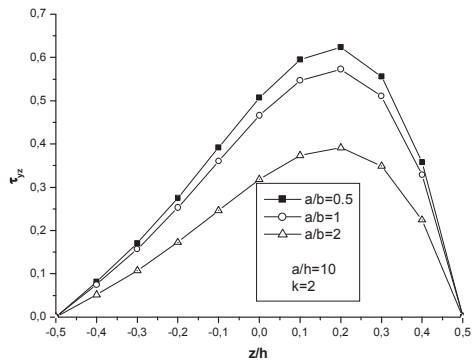

Figure 5: Variation of transversal shear stress (τ_{yz}) through-the thickness of an FGM plate.

tinction between the curves in Figs. 5 and 6 is obvious. As strain gradients increase, the in homogeneities play a greater role in stress distribution calculations. The through-the-thickness distributions of the shear stresses τ_{yz} and τ_{xz} are not parabolic and the stresses increase as the aspect ratio decreases. It is to be noted that the maximum value occurs at $z \cong 0.2$, not at the plate center as in the homogeneous case.

As exhibited in Figs. 7 and 8, the in-plane longitudinal and normal stresses, σ_x and σ_y, are compressive throughout the plate up to $z \cong 0.155$ and then they become tensile. The maximum compressive stresses occur at a point on the bottom surface and the maximum tensile stresses occur, of course, at a point on the top surface of the FGM plate. However, the tensile and compressive values of the longitudinal tangential stress, τ_{xy} (cf. Fig. 4), are maximum at a point on the bottom and top surfaces of the FGM plate, respectively. It is clear that the minimum value of zero for all in-plane stresses σ_x, σ_y and τ_{xy} occurs at $z \cong 0.153$ and this irrespective of the aspect and side-to-thickness ratios.

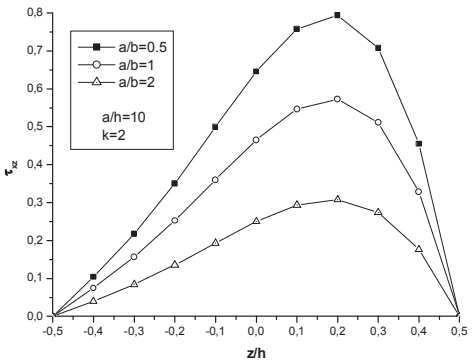

Figure 6: Variation of transversal shear stress (τ_{xz}) through-the thickness of an FGM plate.

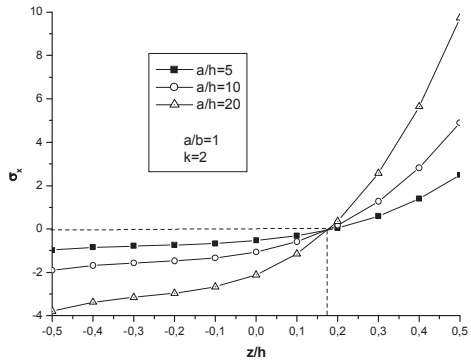

Figure 7: Variation of in-plane longitudinal stress (σ_x) through-the thickness of an FGM plate.

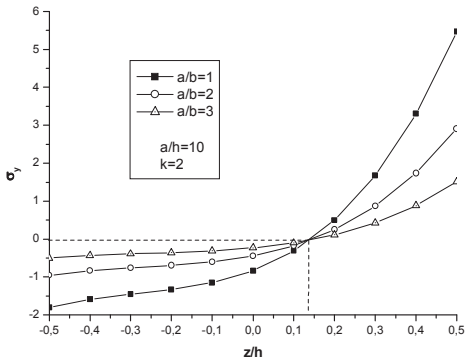

Figure 8: Variation of in-plane normal stress (σ_y) through-the thickness of an FGM plate.

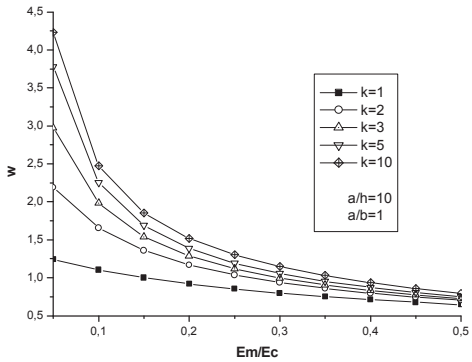

Figure 9: The effect of anisotropy on the dimensionless maximum deflection of an FGM plate.

Finally, the exact maximum deflections of simply supported FGM square plate are compared in Fig. 9 for various ratios of module, E_m/E_c (for a given thickness, $a/h=10$). This means that the deflections are computed for plates with different ceramic-metal mixtures. It is clear that the deflections decrease smoothly as the volume fraction exponent decreases and as the ratio of metal-to-ceramic modules increases.

4 Conclusions

In this study, a new higher order shear deformation model is proposed to analyze the static behavior of functionally graded plates. Unlike any other theory, the theory presented give rise to only four governing equations resulting in considerably lower computational effort when compared with the other higher-order theories reported in the literature having more number of governing equations. Bending and stress analysis under transverse load were analyzed, and results were compared with previous other shear de-

formation theories. The developed theories give parabolic distribution of the transverse shear strains and satisfy the zero traction boundary conditions on the surfaces of the plate without using shear correction factors. The accuracy and efficiency of the present theories has been demonstrated for static behavior of functionally graded plates. All comparison studies demonstrated that the deflections and stresses obtained using the present new higher order shear deformation theories (with four unknowns) and other higher shear deformation theories such as PSDPT and SSDPT (with five unknowns) are almost identical. The extension of the present theory is also envisaged for general boundary conditions and plates of a more general shape. In conclusion, it can be said that the proposed theory NHPSDT is accurate and simple in solving the static behaviors of FGM plates.

References

[1] M. Koizumi, *The concept of FGM*, Ceramic Transactions, Functionally Gradient Materials, 34 (1993), pp. 3–10.

[2] T. Hirai and L. Chen, *Recent and prospective development of functionally graded materials in Japan*, Materials Science Forum, (1999), pp. 308–311.

[3] Y. Tanigawa, *Some basic thermoelastic problems for nonhomogeneous structural materials*, Appl. Math. Mech., 48 (1995), pp. 287–300.

[4] J. N. Reddy, *Analysis of functionally graded plates*, Int. J. Numer. Meth. Eng., 47 (2000), pp. 663–684.

[5] Z. Q. Cheng and R. C. Batra, *Deflection relationships between the homogeneous Kirchhoff plate theory and different functionally graded plate theories*, Arch. Mech., 52 (2000), pp. 143–158.

[6] S. P. Timoshenko and S. Woinowsky-Krieger, Theory of Plates and Shells, McGraw-Hill, New York, 1959.

[7] A. M. Zenkour, *Generalised shear deformation theory for bending analysis of functionally graded plates*, Appl. Math. Model., 30 (2006), pp. 67–84.

[8] M. Şimşek, *Vibration analysis of a functionally graded beam under a moving mass by using different beam theories*, Compos. Struct., 92 (2010), pp. 904–917.

[9] M. Şimşek, *Fundamental frequency analysis of functionally graded beams by using different higher-order beam theories*, Nuclear Eng. Design, 240 (2010), pp. 697–705.

[10] A. Benachour, T. Hassaine Daouadji, H. Ait Atmane, A. Tounsi and S. A. Meftah, *A four variable refined plate theory for free vibrations of functionally graded plates with arbitrary gradient*, Composites part B: Engineering, 42(6) (2011), pp. 1386–1394.

[11] H. H. Abdelaziz, H. Ait Atmane, I. Mechab, L. Boumia, A. Tounsi and E. A. Adda Bedia, *Static analysis of functionally graded sandwich plates using an efficient and simple refined theory*, Chinese J. Aaeronautics, 24(4) (2011), pp. 434–448.

[12] M. Şimşek, *Non-linear vibration analysis of a functionally graded Timoshenko beam under action of a moving harmonic load*, Compos. Struct., 92 (2010), pp. 2532–2546.

[13] H. Werner, *A three-dimensional solution for rectangular plate bending free of transversal normal stresses*, Commun. Numer. Methods Eng., 15 (1999), pp. 295–302.

[14] M. Bouazza, A. Tounsi, E. A. Adda Bedia and M. Meguenni, *Stability analysis of fonctionnally graded plates subject to thermal load*, Adv. Struct. Materials, 15 (2011), pp. 669–680.